Journal of Fundamental and Applied Sciences

Research Article

ISSN 1112-9867

Available online at http://www.jfas.info

SIMULATION OF THE THERMOMECHANICAL LOADS AND CRACK PROPAGATION OF DIFFERENT DIESEL ENGINE PISTON CROWN MATERIALS BY THE XFEM METHOD

M. T. Gherbi[1], A. Nour[2,*], A. Far[3], S. Aguib[2], T. Djedid[2], A. T. Settet[2]

[1]Dynamics of Engines and Vibroacoustic Laboratory, El Oued University, Algeria

[2]Dynamics of Engines and Vibroacoustic Laboratory, F.S.I., Boumerdes University, Algeria

[3]El Oued University, B.P.789, 39000, El Oued, Algeria

Received: 18 Febuary 2019 / Accepted: 27 April 2019 / Published online: 01 May 2019

ABSTRACT

This study concerns the dynamic behavior of the piston of a Deutz F8L413 diesel engine. The objective is to simulate by the extended finite element method (XFEM) the thermomechanical behavior of different piston materials. This study is conducted to evaluate the applied thermal loads and pressure at the end of compression. From a numerical simulation, the stresses acting on the structure and the behavior of the cracked material piston, governed by its global elastic behavior and quantified by the stress intensity factor are determined.

Keywords: materials; cracking; stress; piston; diesel; XFEM.

Author Correspondence, e-mail: abdelkader_nour@hotmail.fr

doi: http://dx.doi.org/10.4314/jfas.v11i2.33

1. INTRODUCTION

The engine piston has been the subject of many studies. In order to solve the problem of compromise between the temperature and the thermal stress of the, Deng et al. [1] have made a multi-objective optimization and a co-simulation to make an optimal design and thermal solutions inside the piston. Söderfjäll et al. [2] performed a high-speed component test bench to evaluate piston ring friction. Wang et al. [3] treated the thermomechanical fatigue behavior (TMF) and the corresponding damage mechanisms to the piston of (Al-Si) alloy, in the temperature ranges of 120-350 °C and 120-425 °C. Dai et al. [4] have done the study of

a new device known as the MTS memory test system, which was designed to measure the temperature of the piston to check the system and the measurement error. The results showed that the MTS has a very high accuracy. Zhang et al. [5] developed a 3D solid model of the piston in the 16V280 diesel engine and a simulation of the steady-state temperature field and the transient state. Dudareva et al. [6] studied experimentally the efficiency of the thermal protection provided by MAO's layer on the piston head. To determine the optimal thickness of the coating, a simulation of the thermal state of the piston using ANSYS Multiphysics was made. Gehlot and Tripathi [7] performed a stable thermal analysis of a ceramic-coated diesel engine piston with holes on its surface. Szmytka et al. [8] performed a thermal fatigue test bench using high frequency induction heating to test the pistons of diesel engines. Rozhdestvensky et al. [9] studied the effect of a thermal insulating coating on a piston of a diesel engine. Using the boundary conditions for heat transfer, a finite element model is applied to evaluate thermal stresses and deformations. Zhao et al. [10] made a detailed thermodynamic analysis to demonstrate the fundamental benefit of HFPE efficiency. Experimental results show that the HFPE combustion process is an almost constant volume process; the efficiency is about 50%.

2. EQUATION SETTING OF THE PROBLEM

2.1 Determination of the temperature distribution

Before determining the distribution of the temperature in the piston, it is supposed that the heat exchanges are purely convective with their environment. The study will be limited to the stationary case. The piston is treated as an isolated three-dimensional system in equilibrium with its environment. The heat flow resulting from the combustion gases is transferred by convection to the bottom piston and then passes through the piston by conduction.

The distribution of the temperature in the piston is given by the Fourier law [11], [12]

$$\vec{q} = -k\overrightarrow{gradT} \quad (1)$$

k is the thermal conductivity coefficient of the heat through the piston, and $\vec{q}$ is the heat flux vector.

Generally the body generates a quantity of internal volumetric heat Q. The inputs and outputs of heat in an elementary cube of dimensions dx, dy, and dz.

The inputs heats in the volume element dv adding the heat Q generated by the volume V are equal to the outputs heat, either

$$Q_x+Q_y+Q_z+QV=Q_{x+dx}+Q_{y+dy}+Q_{z+dz} \quad (2)$$

The inputs heats in the elementary volume dv along the x, y, z directions can be expressed in terms of the heat flux rates, such as

$$\begin{cases} Q_x = \mathrm{d_z}.\mathrm{d_y}.\mathrm{q_x} \\ Q_y = \mathrm{d_z}.\mathrm{d_x}.\mathrm{q_y} \\ Q_Z = \mathrm{d_x}.\mathrm{d_y}.\mathrm{q_z} \end{cases} \quad (3)$$

The rate of the heat flux q is expressed as a function of the temperature gradient and the thermal conductivity coefficient k by the Fourier's law as

$$\begin{cases} q_x = -k_x \frac{\partial T}{\partial x} \\ q_y = -k_y \frac{\partial T}{\partial y} \\ q_z = -k_z \frac{\partial T}{\partial z} \end{cases} \quad (4)$$

On the boundary surfaces, the piston is subjected to the heat transfers by convection, from combustion gas to the lubrication and cooling. These transfers are made on the boundary surfaces and involve the convection coefficients h_i corresponding to each surface.

2.2. Thermomechanical stresses and strains determination

Mechanical equilibrium can be written in different formulations as:

- The complete or global formulation

If we perform the load balance sheet on a finite volume V, we obtain [13]

$$\underbrace{\int_V \vec{f} dV}_{\substack{Volume \\ Force}} + \underbrace{\int_{dV} \sigma \vec{n} da}_{\substack{Surface \\ Force}} = \underbrace{\int_V \rho \vec{\gamma} dV}_{Inertia\ Force} \quad (5)$$

With :

$$\vec{\gamma} = \frac{d\vec{V}}{dt} \quad \text{and} \quad \vec{f} = \rho \vec{g}$$

- The local formulation

If we perform the load balance sheet on an infinitesimal volume, we obtain the local equation of balance [13]:

$$div\sigma + \vec{f} = \rho \vec{\gamma} \quad (6)$$

which is simplified in the static case and becomes

$$div\sigma + \vec{f} = \vec{0} \quad (7)$$

The generalization of this law for a three-dimensional solid (piston) gives the following equilibrium equation

$$\begin{cases} \frac{\partial \sigma_x}{\partial_x} + \frac{\partial \tau_{xy}}{\partial_y} + \frac{\partial \tau_{xz}}{\partial_z} + F_x = 0 \\ \frac{\partial \tau_{xy}}{\partial_x} + \frac{\partial \sigma_y}{\partial_y} + \frac{\partial \tau_{yz}}{\partial_z} + F_y = 0 \\ \frac{\partial \tau_{xz}}{\partial_x} + \frac{\partial \tau_{yz}}{\partial_y} + \frac{\partial \sigma_z}{\partial_z} + F_y = 0 \end{cases} \quad (8)$$

The law of thermoelastic behavior, obtained from the classical Hooke law ε = σ/E, yields

$$\sigma = [D](\{\varepsilon\}_{mec} - \{\varepsilon\}_{th}) \quad (9)$$

With $[D]$ the elasticity matrix for an isotropic material in the case of a three-dimensional solid

$$[D] = \frac{E}{(1+v)(1-2v)} \begin{bmatrix} (1-v) & v & v & 0 & 0 & 0 \\ v & (1-v) & v & 0 & 0 & 0 \\ v & v & (1-v) & 0 & 0 & 0 \\ 0 & 0 & 0 & \frac{1-2v}{2} & 0 & 0 \\ 0 & 0 & 0 & 0 & \frac{1-2v}{2} & 0 \\ 0 & 0 & 0 & 0 & 0 & \frac{1-2v}{2} \end{bmatrix} \quad (10)$$

The vector of thermal strains is written as

$$\{\varepsilon\}_{th} = \begin{Bmatrix} \varepsilon_x \\ \varepsilon_y \\ \varepsilon_z \\ \varepsilon_{xy} \\ \varepsilon_{yz} \\ \varepsilon_{zx} \end{Bmatrix}_{th} = \alpha \Delta T \begin{Bmatrix} 1 \\ 1 \\ 1 \\ 0 \\ 0 \\ 0 \end{Bmatrix} \quad (11)$$

2.3 Formulation of the FEM for the analysis of heat transfer in the piston

The Ritz variational formulation is used for a stationary 3D case [14], [15] and [16].

The temperature distribution T (x, y, z) is the one that minimizes the function

$$I = \frac{1}{2} \iiint \left[K_x \left(\frac{\partial T}{\partial x}\right)^2 + K_y \left(\frac{\partial T}{\partial y}\right)^2 + K_z \left(\frac{\partial T}{\partial z}\right)^2 + 2QT \right] dv \quad (12)$$

Step 1: meshing of the domain V in finite elements (NE: number of elements, NN: number of nodes of the domain V).

Step 2 Approximation Te (x, y, z) on each real element

We have

$$\mathrm{T^e(x,y,z)} = [\mathrm{N(x,y,z)}]\{\mathrm{T^e}\} \quad (13)$$

Shape function (interpolation) associated with the element e

$$[\mathrm{N(x,y,z)}]\left[\mathrm{N_1(x,y,z)N_2(x,y,z)} \ldots\ldots\ldots\ldots \mathrm{N_p(x,y,z)}\right]$$

Where Ni (x, y, z) is the shape function associated with i^{th} node of element. $\{\mathrm{T^e}\}$ is the nodal variable to be determined

$$\{\mathrm{T^e}\}=\begin{Bmatrix} T_1^e \\ T_2^e \\ \cdot \\ \cdot \\ \cdot \\ T_i^e \\ \cdot \\ \cdot \\ T_p^e \cdot \end{Bmatrix}=\left[T_1^e T_2^e \ldots\ldots\ldots T_i^e \ldots\ldots T_p^e\right]^T$$

Step 3: System resolution

$$[K]\{T\}=\{F\} \tag{14}$$

Where

$[K]=\sum_{e=1}^{NE}\left[[K_1^e]+[K_2^e]\right]$ which expresses the global stiffness matrix

$$\{F\}=\sum_{e=1}^{NE}\{F_i^e\} \tag{15}$$

which expresses global loading vector

And

$$\{T\}=\begin{Bmatrix} T_1 \\ T_2 \\ \vdots \\ T_{NN} \end{Bmatrix} \tag{16}$$

which expresses the global nodal vector of domain

The Matrix expressions $[K_1^e],[K_2^e] and \{F\}$ are

$$[K_1^e]=\iiint_{V^e}^{\cdot}[B]^T[D][B]dV \tag{17}$$

$$[K_2^e]=\iint_{S_3^e}^{\cdot}h[N]^T[N]dS_3 \tag{18}$$

$$\{F^e\}=\{F_1^e\}-\{F_2^e\}+\{F_3^e\} \tag{19}$$

With

$$\{F_1^e\}=\iiint_{V^e}^{\cdot}Q[N]^T\,dV \tag{20}$$

Solicitation due to the generated heat Q by the body on a finite element

$$\{F_2^e\}=\iint_{S_2^e}^{\cdot}q[N]^T dS_2 \tag{21}$$

Load due to the heat flux applied to S_2

$$\{F_3^e\}=\iint_{S_3^e}^{\cdot}hT_\infty[N]^T dS_3 \tag{22}$$

Stress due to the convection heat flux applied to S_3 with $[N]=\left[N_1,N_2 \ldots\ldots\ldots\ldots\ldots N_p\right]$ the shape function on a real element,

$[D]=\begin{bmatrix} K_x & 0 & 0 \\ 0 & K_y & 0 \\ 0 & 0 & K_z \end{bmatrix}$ is the material property at the heat transfer,

$[B] = \begin{bmatrix} \frac{\partial N_1}{\partial x} & \frac{\partial N_2}{\partial x} & \frac{\partial N_P}{\partial x} \\ \frac{\partial N_1}{\partial y} & \frac{\partial N_2}{\partial y} & \frac{\partial N_P}{\partial y} \\ \frac{\partial N_1}{\partial z} & \frac{\partial N_2}{\partial z} & \frac{\partial N_P}{\partial z} \end{bmatrix}$ is the matrix of derivatives of shape functions.

2.4. Crack behavior study

2.4.1. Concepts of cracks mechanics

All fatigue cracks are associated with significant stress concentrations. Traditional methods and material properties are not able to describe the behavior of a cracked structure. The fracture mechanics is a path computation of stress and strain fields around a crack **(**Figure 1). For an elastic isotropic material, the stress in the vicinity of a crack can be easily calculated.

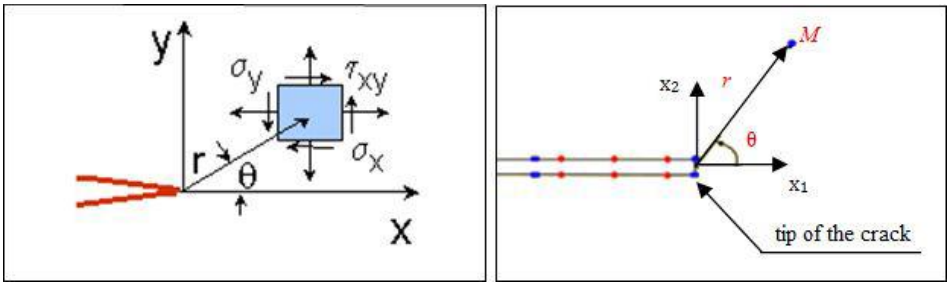

Fig.1. Stresses at the tip of a crack

The stresses at any point θ and r of the crack tip are given by

$$\begin{cases} \sigma_x = \frac{K}{\sqrt{2\pi r}} f_1(\theta) \\ \sigma_y = \frac{K}{\sqrt{2\pi r}} f_2(\theta) \\ \sigma_{xy} = \frac{K}{\sqrt{2\pi r}} f_3(\theta) \end{cases} \quad (23)$$

When the angular variation functions for mode (I) are given respectively by

$$\begin{cases} f_{xx}^I(\theta) = \cos\left(\frac{1}{2}\theta\right)\left(1 - \sin\left(\frac{1}{2}\theta\right)\sin\left(\frac{3\theta}{2}\right)\right) \\ f_{yy}^I(\theta) = \cos\left(\frac{1}{2}\theta\right)\left(1 + \sin\left(\frac{1}{2}\theta\right)\sin\left(\frac{3\theta}{2}\right)\right) \\ f_{xy}^I(\theta) = \cos\left(\frac{1}{2}\theta\right)\left(sin\left(\frac{1}{2}\theta\right)\sin\left(\frac{3\theta}{2}\right)\right) \end{cases} \quad (24)$$

2.4.2. Criterion of propagation and speed

We have three main equations to find the crack and the sudden break:

- The propagation criterion [17]

$$K\ (a, \sigma) = Kc$$

The parameter K is a measure of the magnitude of the stress field in the region of the crack tip and is called the stress intensity factor. Two cracks with the same stress intensity will have the same behavior,

- The speed criterion [18]

$$\frac{da}{dN} = f(\Delta K, R)$$

- The law of Paris [18]

$$\frac{da}{dN} = c(\Delta K)^n$$

$$\Delta K = K_{max} - K_{min} = K_{max}(1 - \frac{\sigma min}{\sigma max}) \quad (25)$$

$$\Delta K = K_{\max}(1 - R)$$

$$R = \frac{\sigma min}{\sigma max}, R = \frac{P_{min}}{p_{max}} \quad (26)$$

Where R is the load ratio, C and n are properties of the material. The propagation of cracks depends on these conditions:

ΔK <ΔKs: No propagation

$\Delta K_s < \Delta K < (1 - R)K_c$ stable propagation

$\Delta K_s < \Delta K < (1 - R)K_c$ unstable propagation

To control the fatigue cracking, it is necessary to know the number of necessary cycles for the initial crack to reach the critical size of instability.

3. Piston simulation methodology

3.1. Objectives

The simulation work is divided into two parts:

The first part concerns the determination of the stationary temperature field in the 3D model of the piston and the thermal stresses. The second part is used to determine the fields of thermomechanical stresses and strains based on the fields of temperature and pressure.

The study will be based on a static analysis of the stresses and strains corresponding to the case of maximum load of the piston at the combustion moment (TDC).

3. 2.Hypotheses of simulation

3.2.a. Geometric hypotheses

This study is applied to the piston of the Deutz F8l413 engine equipping the truck TB230, manufactured by the complex of industrial vehicles (SNVI) of Rouiba (Algeria). For simplicity, we will work directly in the coordinate system related to the geometry of the studied piston.

3.2.b. Assumptions of physical behaviors

i. Descriptions of materials

There are four types of materials whose mechanical and thermal properties are provided by the Table 1.

Table 1. Characteristics of the materials used in the manufacture of pistons

Characteristics	**Stainless steel annealed (SS)**	**Alloy steel (18Cr Mo4)**	**Aluminum alloy (3003-H18)**	**Ductile iron**
Elasticity modulus [N/m^2]	$1.93x10^{11}$	$2.1x10^{11}$	$6.9x10^{10}$	$1.2x10^{11}$
Poisson'ratio	0.3	0.28	0.33	0.31
Density [kg/m^3]	8000	7800	2730	7100
Thermal conductivity [W/m.K]	16.3	14	155	75
thermal expansion coefficient [K]	$1.6x10^{-5}$	$1.1x10^{-5}$	$2.32x10^{-5}$	$1.1x10^{-5}$

The mechanical behavior of materials is considered linear, elastic and isotropic. These properties are the parameters of our simulation [19].

4. Thermal loading conditions of the piston

The combustion produces an important quantity of calorific energy. This quantity of heat is a function of the combustion temperature and heat transfer coefficient of gas. In steady state of the engine, the temperature field is considered to be stationary.

The thermal load in the diesel engine reaches its maximum at the end of the combustion phase. The amount of thermal load quantity has been determined after a previous experimental study, from the thermal load value between 886K and 2659K. The temperature values applied in this study are as follows [20]

$$T_{Min}= 886K \ , T_{Max}= 2659K$$

4.1.Boundary conditions

All nodes which are on the piston axis are fixed in translation and rotation (Figure 2). The displacement and rotation are zero according to the xyz.

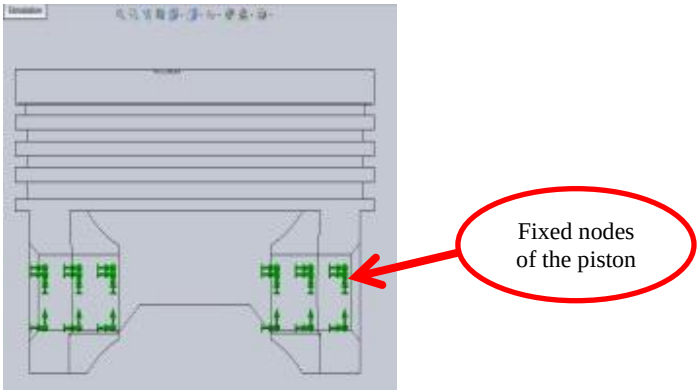

Fig.2. Boundary conditions of the piston

4.2. Meshing

4.2.1. Method of meshing

For the chosen mesh, a free tetrahedral mesh algorithm is used. The mesh is performed automatically using the tetrahedral elements; the structure is meshed in 13322 nodes and 54258 tetrahedrons.

4.3.Results and discussions

4.3.1. Static analysis

4.3.1.a. Piston study without crack under the effect of temperature T = 886 K

After applying a thermal load T = 886 K and a 44,31atm pressure on the piston crown and by changing the piston manufacturing material in each case, we observe the following results (Figure 3).

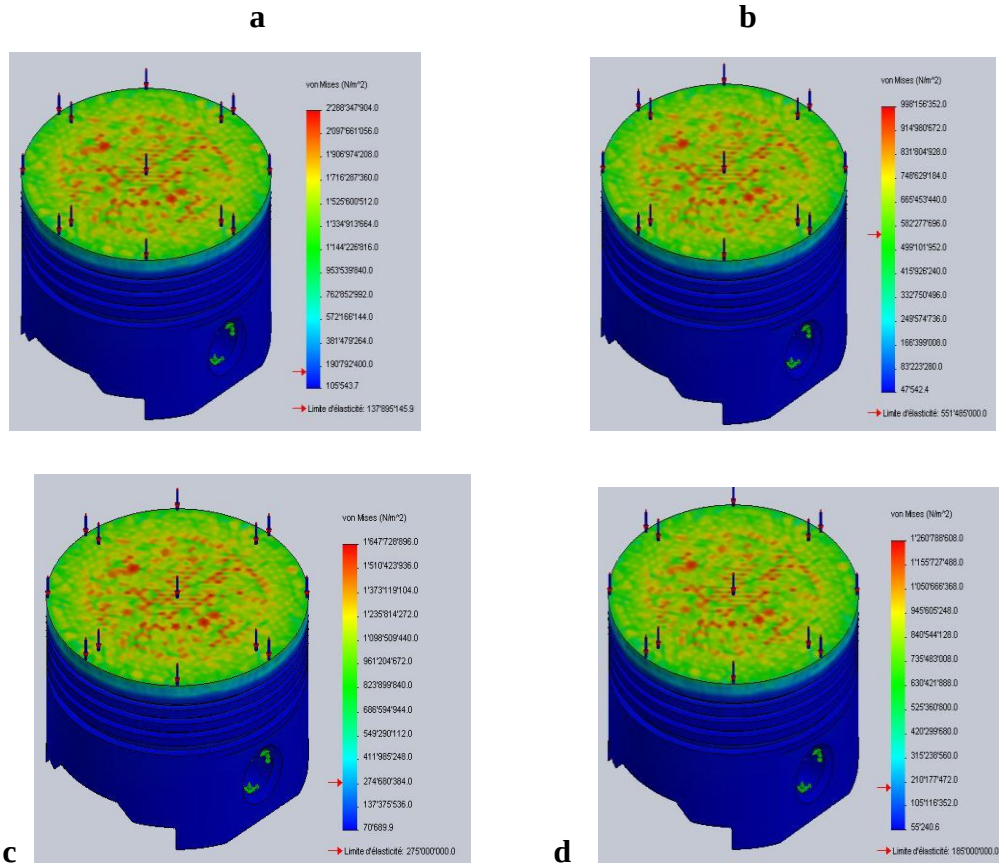

Fig.3. Piston crown stress at T = 886 K for: a) in annealed stainless steel (SS), b) ductile iron, c) alloyed steel (18Cr Mo4), d) Aluminum Alloy (3003- H18)

It is noted that the same propagation of stresses on the piston crown with a different maximum value stresses for each metal.

4.3.1.b. Piston crowns study without crack under the effect of temperature T=2659K

After applying a thermal load of T = 2659 K and a pressure of P = 44.31atm on the piston crown

and changing the piston manufacturing material for each case. When the thermal load applied to the piston crown

Changes according to each metal, the same propagation is observed in all the metals, the value of the maximum stresses vary according to the piston material. Therefore, the piston crown is more sensitive to thermal stresses.

4.3.2. Study of the piston with crack

4.3.2.a. Create a crack on the piston head

A piston crown crack is created with dimensions (Length: 60 mm, Width: 0.5mm, Depth: 0.5mm) by the following steps:i Step 1: drawing of the crack (select the surface to create a crack).ii. Step 2: The 3D crack shape. Create the crack and extend the 2D plan design to the 3D, using the cutting tool to remove material.

After applying a thermal load of T = 886 K and a pressure of P = 44.31atm on the piston crown and changing the piston manufacturing for each case material, we observe the following results (Figures. 4 and 5).

4.3.2.b. Piston crown *with crack under the effect of temperature T = 886 K*

After the design steps, the final shape of the piston crown with crack is obtained.

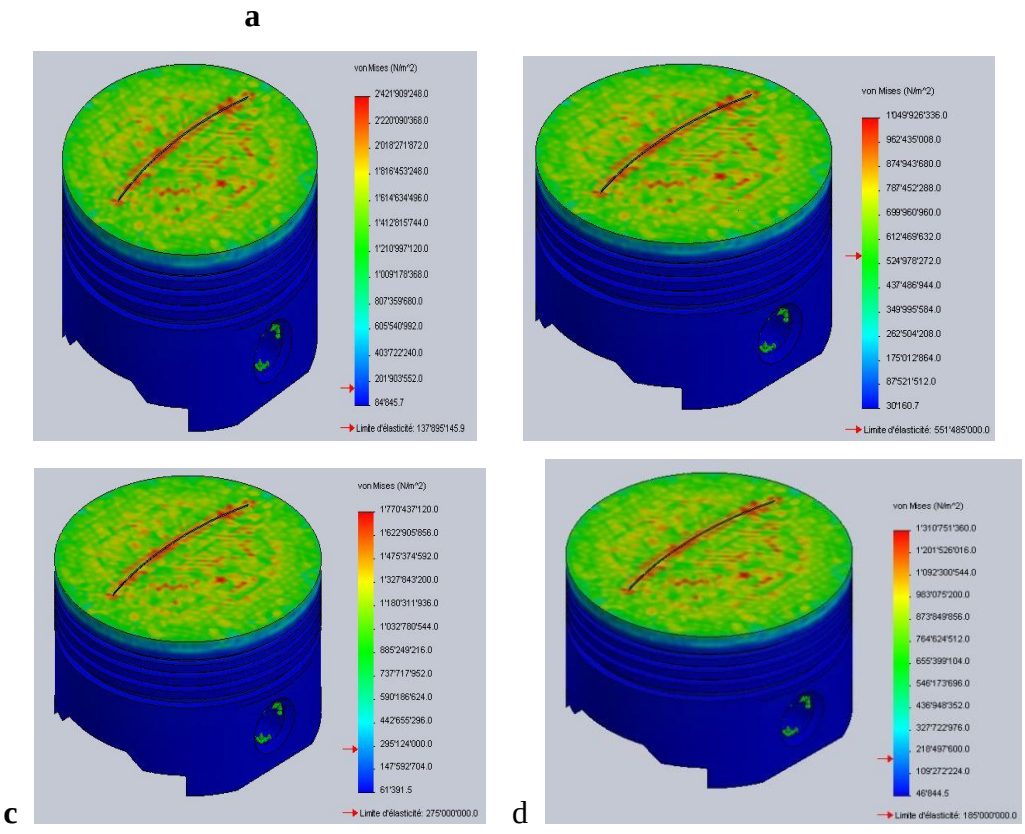

Fig.4. Thermal stress of piston crown at T = 886 K in: a) annealed stainless steel (SS), b) ductile iron, c) alloy steel (18Cr Mo4), d) aluminum alloy (3003-H18)

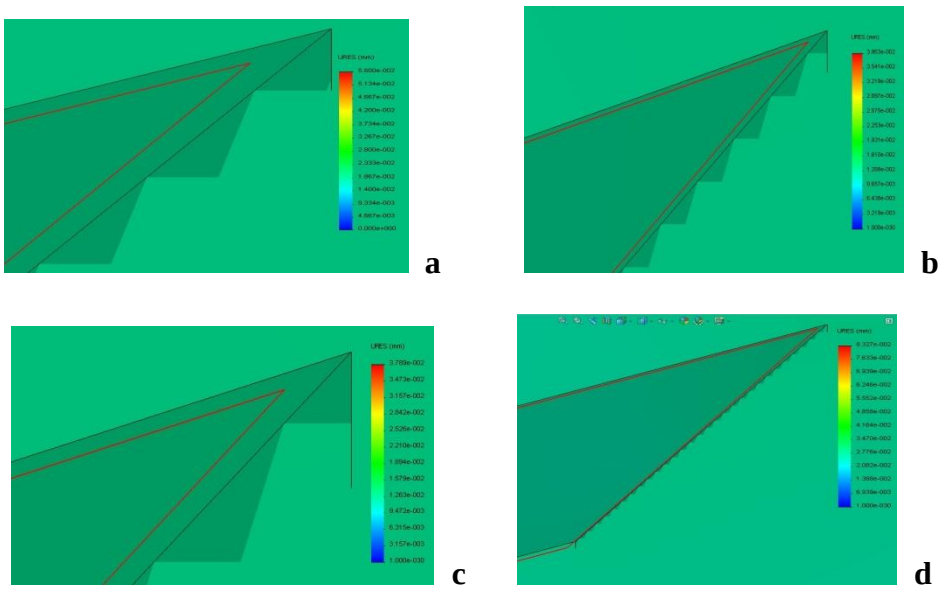

Fig.5. Piston crown crack propagation T = 886 K for: a) annealed stainless steel (SS), b) ductile iron, c) alloy steel (18Cr Mo4),d)) aluminum alloy (3003-H18)

4.3.2.d. Crack piston study under the temperature effect of T = 2659 K

After applying the thermal load of 2659 K on the four previous materials, we can make the same observations, furthermore the stresses increase for each material around the contour of the cracks. Also, the value of the crack propagation increases according to the thermal load and the propagation direction varies according to these latter.

The stresses of the piston with and without crack under thermal load impact are shown in Figures 6 and 7. Note that the stresses in the cracked piston are higher compared to those of the piston without crack whatever the mechanical characteristics of the material.

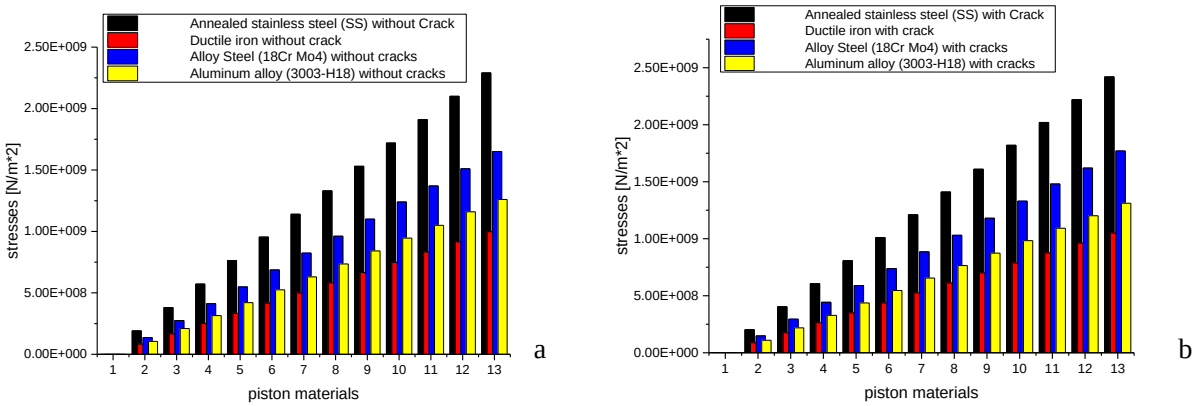

Fig.6. Stresses vs piston crown materials under the effect of a thermal load of 886K: a) without crack, b) with crack

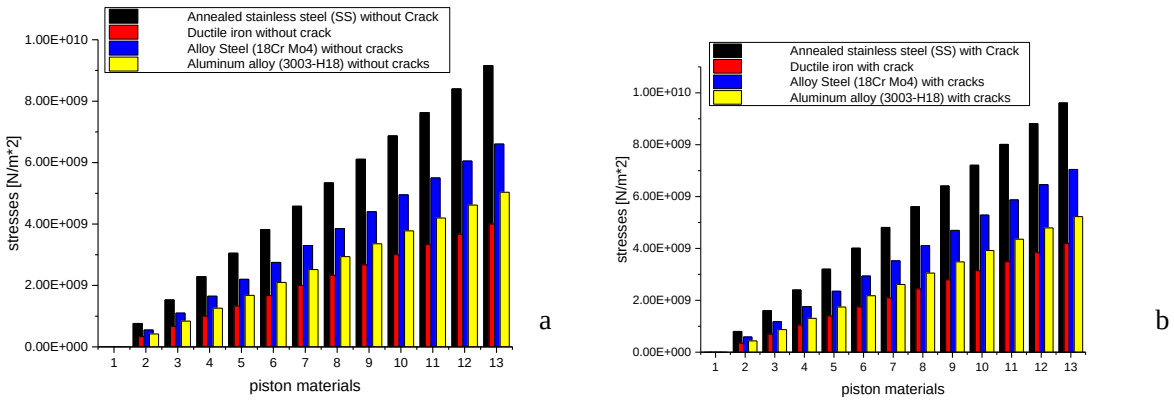

Fig.7. Stresses vs piston crown materials under the effect of a thermal load of 2659K: a) without crack, b) with crack

The impact of thermal loads is also significant on the crack propagation (Figure 8).

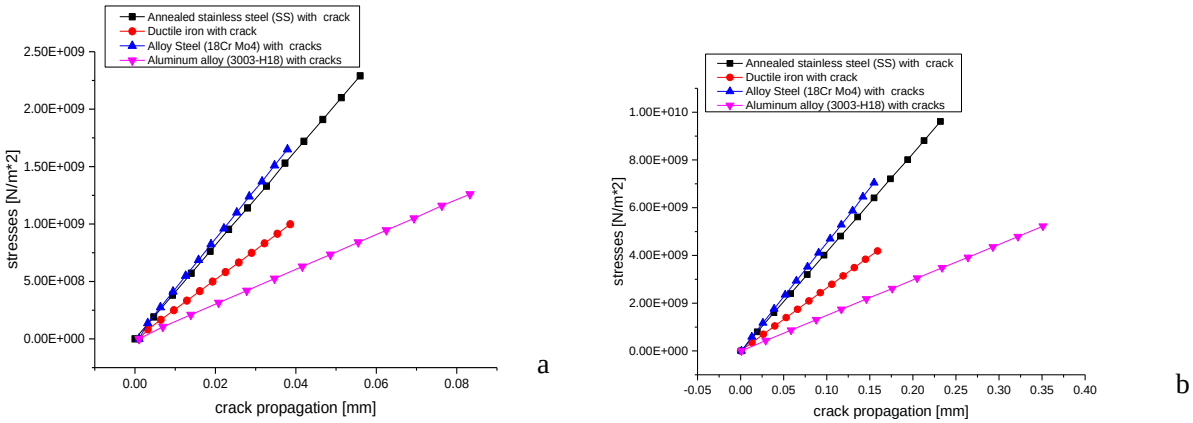

Fig.8. Crack Propagation vs the loading heat of the piston crown at: a) T = 886K., b) T=2659K

The crack propagation increases with the increase of the stresses, because the stresses and displacements change according to the applied thermal load. The annealed stainless steel (SS) and aluminum alloy (3003-H18) are more affected by the thermal load represented in Figure 8.

5. CONCLUSION

The mechanical and thermal properties are the essential parameters for the manufacture of the engine piston. For engines subjected to severe regimes, where the combustion parameters

(temperature and pressure) are important, the thermal stresses have an important role as the mechanical stresses. This requires an additional piston crown shape study and its lubrication and cooling circuit.

The piston modeling requires an appropriate mesh, a sensitivity analysis to obtain the optimal size of the element and the accuracy determination of the solution. The behavior of the cracked material, governed by its global elastic behavior is quantified by the factor of stress intensity K. The temperature impact on the piston material highlights a large number of parameters of the linear fracture mechanics. This is based on the thermoelastic analysis of thermal stresses at the crack tip, to characterize the strength of materials. There are three parameters that control the cracks propagation: the thermal stresses, the size of the crack and the tenacity of the material. The crack propagation increases with the increase of the stresses according to the applied thermal load. The annealed stainless steel (SS) and aluminum alloy (3003-H18) are more affected by the thermal load.

This study allowed us to appreciate the importance of the piston crown profile, the temperature which increases the vulnerability of piston crown cracking, the maximum stress values and the piston crown crack behavior to select the most adequate material.

REFERENCES

[1] Deng X, Lei J, Wen J, Wen Z, Shen L. Multi-objective optimization of cooling galleries inside pistons of a diesel engine, Applied Thermal Engineering. (132)March 441- 449. Matched ISSN : 1359-4311. (2018)

[2] Söderfjäll M, M.Herbst H, Larsson R, Almqvist A. Influence on friction from piston ring design, cylinder liner roughness and lubrican properties. December (2017) 272-284(116).

[3] Wang M, Pang J C, Zhang M X, Liu H Q, Li S X, Zhang Z F. Thermo-mechanical fatigue behavior and life prediction of the Al-Si piston alloy. Materials Science and Engineering. A (715) 7 February 62-72. Matched ISSN : 0921-5093 (2018).

[4] Dai H, Huang R, Li G, Tang J, Huang S. Memory test system for piston steady-state temperature measurement. Applied Thermal Engineering. (110)5 January 436-441. Matched ISSN : 1359-4311 (2017).

[5] Lu Y, Zhang X, Xiang P, Dong D. Analysis of thermal temperature fields and thermal stress under steady temperature field of diesel engine piston. Applied Thermal Engineering. (113) 25 February 796-812. Matched ISSN : 1359-4311 (2017).

[6] Szmytka F, Salem M, Rézaï-Aria F, A.Oudin. Thermal fatigue analysis of automotive Diesel piston: Experimental procedure and numerical protocol International Journal of Fatigue. (73) April 48-57. Matched ISSN : 0142-1123 (2015).

[7] Yu.Dudareva N, R.D.Enikeev, V.Yu.Ivanov. Thermal Protection of Internal Combustion Engines Pistons. Procedia Engineering. (206) 1382-1387 (2017).

[8] Gehlot R, Tripathi B. Thermal analysis of holes created on ceramic coating for diesel engine piston. Case Studies in Thermal Engineering. (8) September 291-299 (2016).

[9] Rozhdestvensky Y, Lazarev E, Doikin A. Effect of the Heat Insulating Coating of the Piston Crown on Characteristics of the “Piston-Cylinder Liner” Pair Procedia Engineering. (150) 541-546 (2016).

[10] Zhao Z, Wang S, Zhang S, Thermodynamic and energy saving benefits of hydraulic free-piston engines. Energy Volume 102, 1 May 650-659 (2016).

[11] RANC N. 'Couplage thermomécanique' Technique de l'Ingénieur, référence AF5 042, juil., 2003.

[12] Singiresu S. Rao. 'The finite element method in engineering fourth edition’, Elsevier Science & Technology Books, (2004).

[13] Reddy J N and D.k Garthing.,’ The finite element method in heat transfer and fluid dynamic’, Edition C RC press (1994).

[14] Reddy J N , 'Finite element method introduction', Edition Mc Graw-Hill 1993.

[15] David .V. hutton.,’ Fundamental of finite element analysis Edition MacGraw- Hill, NY 10020, New York (2004).

[16] Liu G R, Quek. S,'The Finite Element Method:A Practical Course', Butterworth-Heinemann, Linacre House, Jordan Hill, Oxford OX2 8DP,(2003).

[17] Christian CLOS,’ Technologie des moteurs alternatifs à combustion interne 'technique d’ingénieur, volume B2, (2000).

[18] Christian CLOS,’ Technologie des moteurs alternatifs à combustion interne technique

d'ingénieur, volume B2, (2000).

[19] LEMAIRE M, « Moteurs À Combustion Interne », Polycopié du cours des moteurs thermiques, École Centrale de Nantes, Nantes (2003).

[20] MORKOS M. « Moteurs À Combustion Interne », Polycopié du cours des moteurs thermiques, U. Libanaise, Beyrouth 2002. ourth edition', Elsevier Science & Technology Books, (2004.

How to cite this article:
Gherbi MT, Nour A, Far A, Aguib S, Djedid T, Settet AT. Simulation of the thermomechanical loads and crack propagation of different diesel engine piston crown materials by the xfem method. J. Fundam. Appl. Sci., 2019, *11(2), 1061-1075.*